Characterization of expanded polystyrene-ferrocement geomat

Fauziah Ahmad, Muhamad Hisyam Halim
Universiti Sains Malaysia and MyIGS, Malaysia

Vivi Anggraini
Mobash University Malaysia, Malaysia

ABSTRACT: In this study, preventive measures for landslide activity are being addressed and 8-shaped geomat is proposed to curb this problem. The mechanical properties such as resistance to compression, flexural and pull out resistance of 8-shaped expanded polystyrene (EPS)-ferrocement are to be determined. End result is compared to previous study made of different materials. 8-shaped geomat is developed by using hand plaster method. Two types of mixture proportion are produced namely as EPB10 and EPB30 signifying that the mortar's sand mix proportions are partially replaced with 10% and 30% of expanded polystyrene beads respectively. Compression and flexural is tested with Universal Testing Machine (UTM). Pull out test is performed in pull out box with sand as the backfill material. Test results show that both EPB10 and EPB30 have similar test results. Comparing to 8-shaped geomat made of fiberglass, used tires and ferrocement, expanded polystyrene based ferrocement has similar compressive strength, lower flexural force and lower pull out force.

Keywords: 8-shaped geomat, expanded polystyrene, expanded polystyrene beads, ferrocement, compressive strength, flexural force, pull out force

1 INTRODUCTION

EPS concrete is the mixture of cement, sand and expanded polystyrene beads. From ACI Committee (2003), the concrete shall achieve minimum 17MPa compressive strength at 28th day to qualify as structural lightweight concrete. Park and Chisholm (1999), performed study on strength and drying shrinkage of recycled EPS concrete and proved similar strength for both waste granulated polystyrene and polystyrene beads concrete. Saradhi Babu et al. (2005), indicated the EPS concrete behaved like cushioned and energy absorbing materials. Studies of different factors such as water to cement ratio, density, volume of EPS, admixtures are reported. Babu et al(2005), Xu et al (2012)

Slope stabilization and soil erosion control can be achieved by biotechnical and soil bioengineering approach reported by Gray and Sotir (1990). Other alternatives are the utilization of geosynthetic materials such as geotextiles, geogrids, geonets and others. Lekha (2005) reported that natural geotextiles made of natural fiber are preferred than synthetic geotextiles due its ability to prevent excessive heating and seeds protection at early age for vegetative growth. New products named as 8-mat system or 8-shaped geomat are produced for these purposes as well. There are studies on 8-shaped geomat made of different materials such as fiberglass, used tires and ferrocement, Yohanes(2010). Similar application is practised for hard armor erosion control system particularly articulating concrete block by Matthew Stovall and King. (2011)

2 MATERIALS AND TEST METHODS

2.1 *Materials*

Sand was used for the mix is graded conforming to BS 812-102; 1990. For the mortar cubes, EPS used in the mortar mix are expanded polystyrene beads (EPB) and waste granulated polystyrene (WGP). Expanded polystyrene beads are spherical and have mean particle size of 5.16mm. While waste granulated polystyrene are made of unused EPS slabs reduced to irregular size and shape using grater and hand means.

Mix proportion used for control mix is proportioned as cement: sand: water = 1: 2.5: 0.45 with target mean strength at 28th day is 30MPa for normal concrete strength and consistency is maintained below 150mm flow diameter. Sand in ferrocement mortar is replaced by two different types of expanded polystyrene, which are expanded polystyrene beads (EPB) and waste granulated polystyrene (WGP) varying from 10% to 30%. The mortar mix is proportioned using absolute volume method as prescribed in ACI Manual of Concrete Practice, Part 1.(1999) Consistency of the fresh mix is determined in accordance to procedures prescribed in BS EN 1015-3-1999. The mortar cubes mixture proportions is shown at Table 2.1.

Table 2.1 Mortar mixture proportions

Constituents	Mixture proportions		
Expanded polystyrene beads (EPB)	EPB10	EPB20	EPB30
Cement	1	1	1
Sand	2.25	2	1.75
Water	0.45	0.45	0.45
EPS	0.25	0.5	0.75
Waste granulated polystyrene (WGP)	WGP10	WGP20	WGP30
Cement	1	1	1
Sand	2.25	2	1.75
Water	0.45	0.45	0.45
EPS	0.25	0.5	0.75

2.2 *8-shaped geomat*

The expanded polystyrene beads (EPB) are selected to produce 8-shaped EPS geomat. Two different EPB mixture proportions of 10% and 30% are used to produce the 8-shaped EPS geomat named as EPB10 and EPB30 respectively. Wire mesh used is galvanized welded square wire mesh, 1.25mm in diameter and 8.75mm × 8.75mm aperture. EPS beads have mean particle size of 5.16mm. Cement applied is ordinary Portland cement and is purchased from local distributor. Clean tap water is used and sand is natural river sand with 2700 kg/m^3. 1000 mm length and 140 mm width of wire mesh is cut to form the reinforcement layer. The wire mesh is then tied from end to end to form a circular loop.

2.3 *Tests methods*

To determine the compressive strength of EPS mortar, 50mm×50mm×50mm cubes are prepared. Mortar cubes are cured in the mold for 24 hours prior remolding process and are cured in water tank till the age of testing as recommended in BS 1881-111:1983.Three samples will be tested at the testing age of 7-day, 14-day and 28-day. Dry mass of mortar cubes are taken to measure their density.

For 8-shaped geomat a 3 point load test is used to determine the flexural strength of 8-shaped EPS geomats using Universal Testing Machine (UTM). Firstly, the distance of two solid steel shafts acting as support is measured and placed at a distance of 250mm apart from each other. Next, the geomat sample is marked with two lines indicating a distance of 125mm to the left and right from the center of geomat sample. Thirdly, the geomat sample is placed on the solid steel shafts with the lines aligned with the marking lines craved on both of the center solid steel shaft. Fourthly, the load cell is gradually lowered until it touches the geomat sample. Under loading condition, geomat sample is loaded with 1mm/minute deflection rate until it fails. The flexural test is repeated with two sets of EPS geomat samples of 10% and 30% content with each set contains two EPS geomat samples.

As for compression test is conducted to determine compressive strength of 8-shaped EPS geomats using UTM. Firstly, a thin rectangular shape metal plate is laid on the base of UTM. Next, the geomat

sample is placed on the metal plate followed by laying a steel block on top of the geomat sample to impose uniformly distributed load on it. The steel block has a thickness of 38mm, length of 470mm, width of 130mm and weight of 174kN. Thirdly, the load cell is gradually lowered until it makes contact with the steel block. The geomat sample is then subjected to controlled rate of vertical deformation of 1mm/minute until it fails. The compression test is repeated with two sets of geomat, which are EPB10 and EPB 30 with each set contains two samples.

The aim of pull out test is to stimulate the pull out resistance mechanism along the soil reinforcement interface. Laboratory pull out test is performed to determine pull out resistance of 8-shaped EPS-ferrocement geomats embedded in sandy soil. The pull out resistance value is correlated to the overburden loads subjected during the tests giving relationships between the pull out resistance and overburden load.

For single arrangement of 8-shaped EPS-ferrocement geomat, the EPS-ferrocement geomat sample is laid on a layer of compacted sand soil. The thickness of the base layer is adjusted so that the center height of the EPS-ferrocement geomat matches wirh the position of modified clamp. Next, second layer of sand soil is filled into the box up to the top of the EPS-ferrocement geomat level. After that, an amount of 100 kg of sand is weighted and poured onto the second layer and is being levelled. Finally, the weight of 100 kg is laid on the final layer acting as the overburden load equal to 0.981kN. The overburden load is varied by addition of steel weights on top of the final sand layer.

3 RESULT AND DISCUSSION

3.1 *Compression test for mortar cubes*

The mortar mix result showing density, density reduction and compressive strength at 7-day, 14-day and 28-day is shown in Table 3.1.

Table 3.1 Tabular result of EPS beads and waste granulated polystyrene mortar cubes

Samples		Density (kg/m^3)	Density Reduction (%)	Compressive Strength (MPa)		
				7th	14th	28th
Control mix		2283	-	32.0	36.0	39.3
EPS Beads (EPB)	EPB10	2111	7.5	24.2	24.8	25.7
	EPB20	1931	15.4	14.6	15.9	16.1
	EPB30	1759	23.0	9.2	9.5	10.6
Waste Granulated Polystyrene (WGP)	WGP10	2218	2.9	26.7	27.3	28.8
	WGP20	2093	8.3	20.0	20.6	22.2
	WGP30	1795	21.4	11.4	11.9	13.5

The compressive strength of EPS concrete mix is a function of density which is the same case for other types of lightweight aggregate concrete. The cubes are tested for their compressive strength at 7 day, 14 day and 28 day. 3 cubes are tested at each age. For control mix, the target mean strength 30MPa is achieved at 7 day which is 32.0MPa. The compressive strength of both EPS beads and waste granulated polystyrene mortar increases with age from 7-day to 28-day. Both mortars exhibit rapid growth of compressive strength at early stage. The result shows that at 7-day, both types of mortars had achieved 85 to 94% of compressive strength at 28-day. As the amount of EPS increases, the compressive strength and density decreases for both types of mortar. With 30% sand replacement with EPS, the density reduction is up to 23.0% and 21.4% for EPS beads mortar and waste granulated polystyrene mortar respectively.

To compare both EPS beads and waste granulated polystyrene mortar, Waste granulated polystyrene mortar has slightly higher compressive strength than EPS beads mortar. As EPS is measured in terms of volume instead of weight due to its lightweight properties, a specific volume amount of waste granulated polystyrene will be much lesser as it has irregular size and shapes at which the waste granulated polystyrene cannot arrange themselves in a dense manner. Compared to EPS beads having spherical shapes, the beads particles are capable of packing closely to each other and thus results in higher specific volume amount. Eventually higher percentage of EPS amount results in reduction in compressive strength. Figure 3.1 to Figure 3.3 shows effect of EPS content on density of mortar and strength development for EPS beads and waste granulated polystyrene mortar.

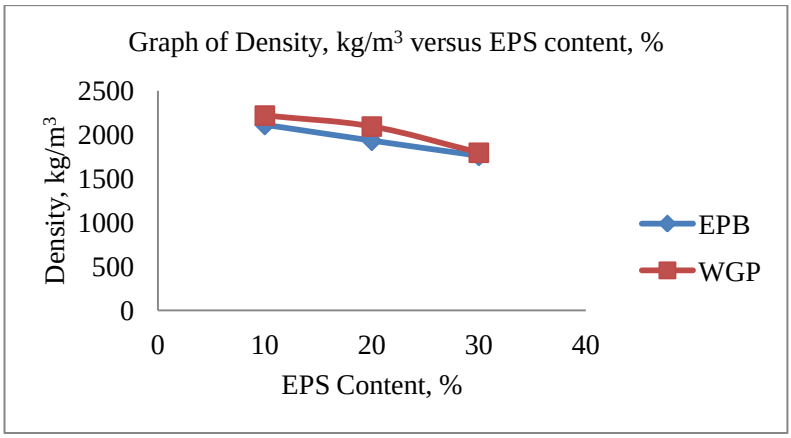

Figure 3.1 Effect of EPS content on density of mortar

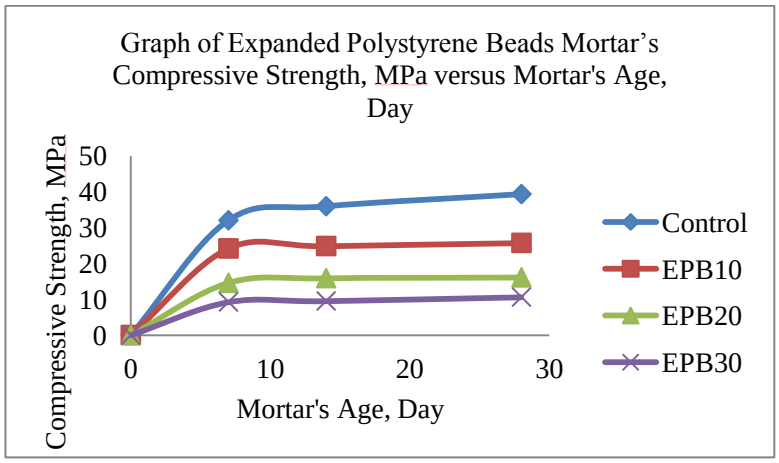

Figure 3.2 Strength development of EPS beads mortar

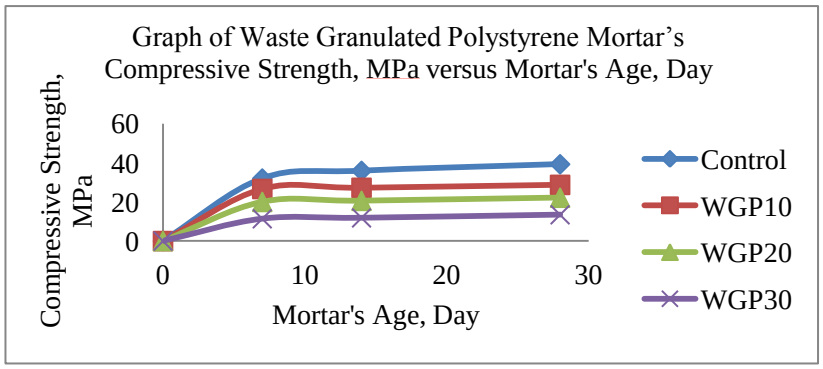

Figure 3.3 Strength development of waste granulated polystyrene mortar

3.2 *Flexural test*

3 point load test is used to determine the flexural strength of 8-shaped geomat instead of 4 point load test. It is noticed that the 8-shaped geomat used for EPS-ferrocement is smaller in size with the geomat length about 450mm. Previous study using ferrocement geomat has twice the size with the length of about 927mm. For 4 point load test, the reduced distance between bottom support and distance between two upper steel shafts for small 8-shaped geomat results in shear failure instead of flexure failure. Thus, 3 point load test is proposed for small 8-shaped geomat to ensure that the sample has sufficient distance for flexure failure to occur.

Unlike beam with uniform cross sectional area, the 8-shaped geomat are unable to compute the flexural strength using derieved equation. Thus, the result is expressed in first crack force and flexural force. In the test, the load-deflection curve of the 8-shaped geomat samples show distinct linear behavior up to force at first crack except samples EPB101 and EPB301. After the cracking load, the curves continue on showing linear behavior until the ultimate flexural force at which the samples fail. It is seen

that the crack formation for the tested samples propagate from the bottom part of the samples indicating that the geomats are weak at tension zone and fail due to flexure moment. Visible minor deformation can be seen at the upper part of samples due to apply of load cell. As flexure load increases, the crack transverses across the samples from bottom to top.

The ultimate flexural force for EPS-ferrocement is in the range of 5.66 to 8.21kN. The force is much lower compared to ultimate flexural force of 32.56-36.59kN for ferrocement geomat. This might be due to the ultimate flexural force for ferrocement is governed by the number of layers of wire mesh reinforcement embedded within the mortar matrix. The small size of EPS-ferrocement geomat only uses single layer of wire mesh. For previous study of ferrocement geomat, two layers of wire mesh are used. As both EPB10 and EPB30 samples exhibits similar ultimate flexural force, it can be said that the ultimate flexural force does not depend much on mortar matrix material or the mixture proportions. Figure 3.4 and Figure 3.5 shows the fexural load-deflection curves of EPB10, EPB30 8-shaped EPS-ferrocement geomat and the formation of cracks due to flexural loading.

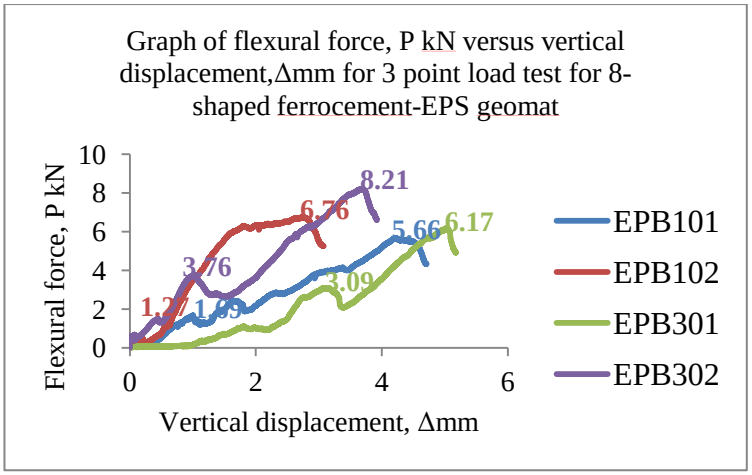

Figure 3.4 Flexural load-deflection curves of EPB10 and EPB30 8-shaped EPS-ferrocement geomat

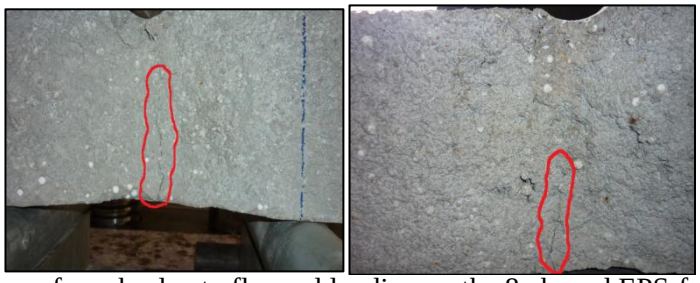

Figure 3.5 Formation of cracks due to flexural loading on the 8-shaped EPS-ferrocement geomat

3.3 *Compression test*

Compressive strength for 8-shaped geomat can be computed by dividing the maximum compression force by average plane's surface area subjected to compression. The test result shows that the compressive strength of both EPB10 and EPB30 EPS-ferrocement geomat has similar compressive strength ranges from 4.14 to 5.57MPa. The ultimate compressive strength result is similar to previous study using ferrocement, where it records the ultimate compressive strength of 4.81 and 5.77MPa. For the case of EPB10 EPS-ferrocement geomat, the compressive strength is only about 16.7 to 17.1% of the 14-day EPB10 mortar cubes compressive strength. EPB30 EPS-ferrocement geomats achieve 44.3% to 66.0% of the 14-day EPB30 mortar cubes compressive strength. Figure 3.6 shows the compression-vertical deformation of EPB10 and EPB30 8-shaped EPS-ferrocement geomat.

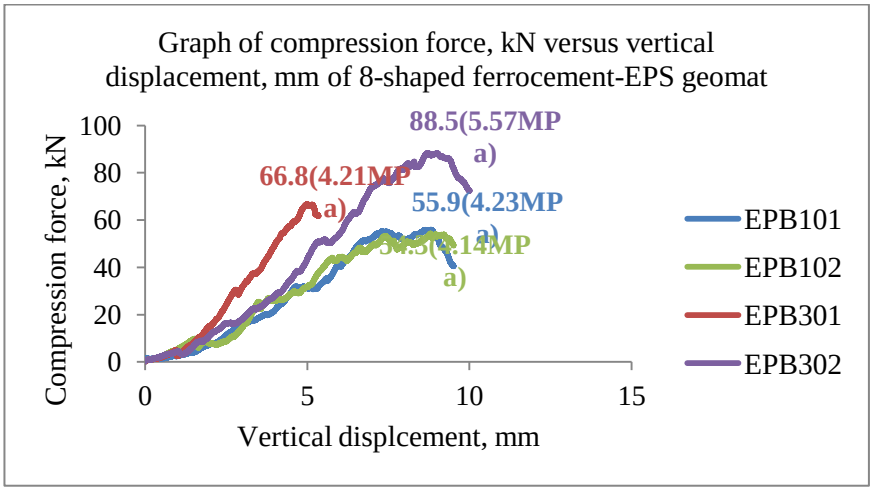

Figure 3.6 Compression-vertical deformation of EPB10 and EPB30 8-shaped EPS-ferrocement geomat

There are a few potential factors that can affect the compressive strength of the EPS-ferrocement geomats. Firstly, the formation of shrinkage cracks during hardening and maturing stage might serves as the weak planes which become potential spot for compression failure or induced shear stress to occur. Secondly, hand-made EPS-ferrocement geomat has irregular dimensions. The irregular dimensions region induces bucking moment when geomat is subjected to compression force. The buckled part undertakes more stress than any other part of member. This leads to failure cracks of the member initiated at the buckled part. Failure cracks in the direction of compression force across the geomat sample would have observed if the geomat involves zero buckling during compression.

Figure 3.7 shows the failure pattern of the tested EPS-ferrocement geomats. In Figure 3.7(a), the red circle region emphasize that the geomats fail at the upper part region due to buckling action. The buckling action creates localized cracks concentrated at the upper part of the compressed sample. These cracks elongate from the cover or surface of EPS-ferrocement mortar until they reach the wire mesh causing failure at the wire mesh as shown in Figure 3.7(b). The wire mesh remains intact within the geomat showing good bonding strength. At the same time, wire mesh also serves as weak plane as compression force continue to exert load on wire mesh after the mortar cover is torn off causing wire mesh to invert inward and outward. In Figure 3.7(c), it is seen that the failure crack propogates across the geomat in the direction of compression force indicating the load transfer from the load cell to the base of the geomat. Judging from the arrangement and position of wire mesh in the geomat as the skeleton or core body of the 8-shaped geomat as well as the lack of sufficient cover, it is believed that wire mesh contribute significantly to the compressive strength of 8-shaped geomat more than the mortar matrix of 8-shaped geomat.

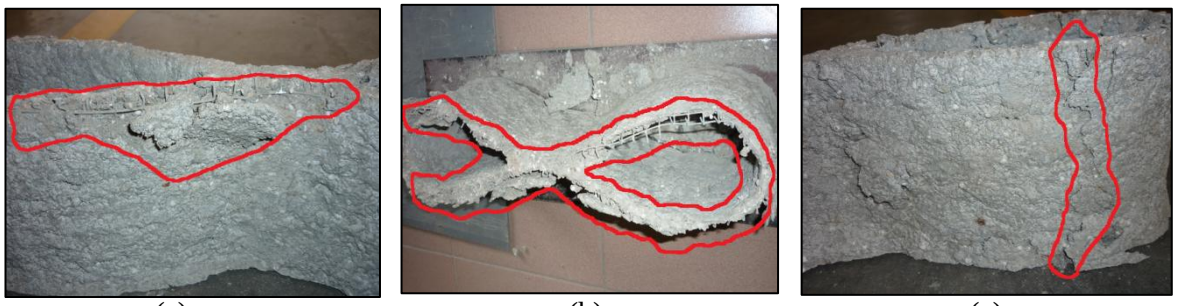

(a) (b) (c)

Figure 3.7 Failure patterns of compressed 8-shaped EPS-ferrocement geomat

3.4 *Pull out test*

The geosynthetics pullout resistance is a function of skin friction, generated between the solid portion of the reinforcement and the soil and the passive resistance mobilized in correspondence of the bearing members placed transversely to the pullout force direction. In particular, the main soil parameters that influence the pullout behavior are the same that typically affect the dilatancy such as relative density, the grain size distribution (in relation to the geogrid mesh size) and the vertical effective confining stress. About the reinforcement, the geometry and thickness of the transverse elements, the mesh size (in term of spacing between elements) and the longitudinal and transversal members' stiffness play an important role in the mechanical behavior of geogrids.

For 8-shaped EPS-ferrocement geomats which act as soil reinforcing material, the geomats will be tested corresponds to the arrangement of single geomat parallel with the pullout force.

Figure 3.8 and Figure 3.9 show pull out resistance force with pull out distance and overburden loads ranging from 0.981kN to 3.924kN for EPB10 and EPB30 8-shaped EPS-ferrocement geomats. Most of the geomat samples show the same curve pattern. All the geomat samples show curve of increasing pull out resistance gradually with increasing pull out distance due to the dense arrangement of undisturbed soil particles with likely interlocking and frictional surface interface contact between the soil particles and the ferrocemet-EPS geomat. The increasing pattern of pull out resistance force continues until it reaches point at which maximum pull out resistance is attained. Beyond this point, the increasing pull out distance is followed by decreasing value of pull out resistance force. The backfill material for pull out test for this study is sand. As sand is cohesionless, thus the friction between the geomat and soil medium is less results in lower pull out resistance. Previous study of pull out test using crusher run has higher pull out resistance force.

The linear relationship of maximum pull out resistance varies proportionally with overburden load is shown in Figure 3.10. The result shows that both EPB10 and EPB30 exhibit similar pull out resistance force with EPB10 have slightly higher pull out resistance force.

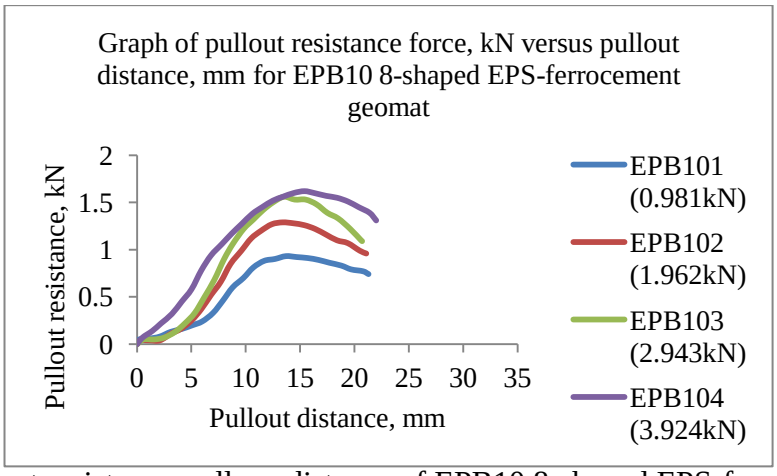

Figure 3.8 Pull out resistance-pull out distance of EPB10 8-shaped EPS-ferrocement geomat

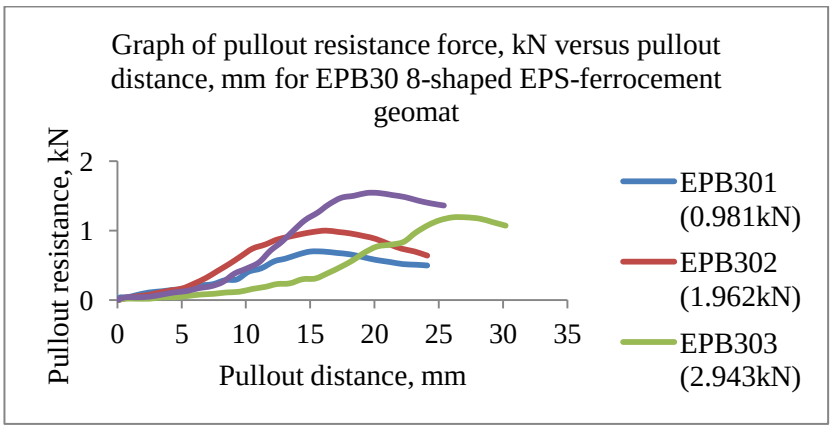

Figure 3.9 Pull out resistance-pull out distance of EPB30 8-shaped EPS-ferrocement geomat

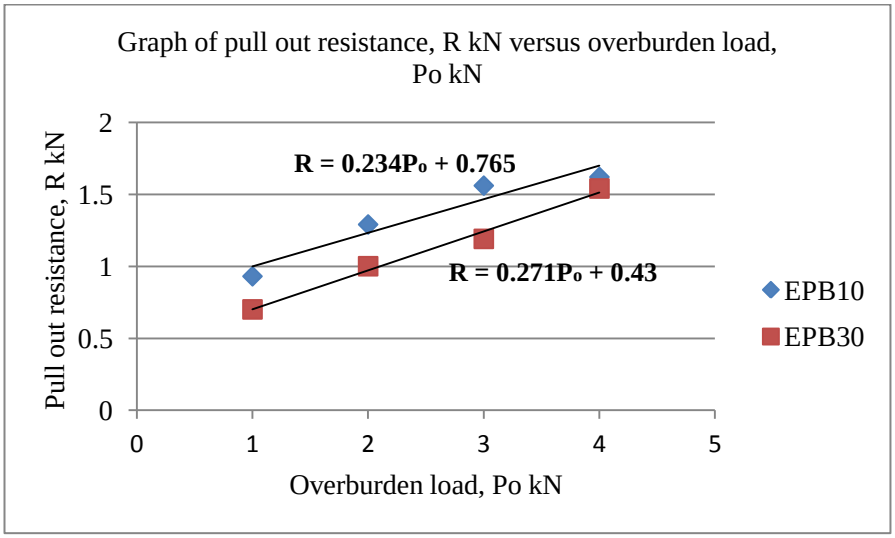

Figure 3.10 Linear relationships of overburden load with maximum pull out resistance for EPB10 and EPB30 8-shaped EPS-ferrocement geomat

3.5 *Comparison among 8-shaped geomats made of different materials*

Table 3.2 shows the comparison among the three types of 8-shaped geomat made of varying materials such as ferrocement, used tires and fiberglass.

Table 3.2 Comparison among EPS-ferrocement geomat with ferrocement geomat, used tires geomat and fiberglass geomat

Properties	EPS-ferrocement	Ferrocement	Used tires	Fiberglass
Tensile force, kN	**5.58-8.21 (flexural)**	**32.56-36.59 (flexural)**	**14-20**	**21.7**
Compressive strength, MPa	**4.23-5.57**	**4.55-5.77**	**None**	**None**
Pull out resistance, single kN	**1.56**	**4.55**	**18.94**	**16.89-21.58**
Weight, kg/unit	**4.0 to 4.2**	**30-32**	**Less than 1kg**	**Less than 1 kg**

4 CONCLUSIONS

Based on the laboratory result and analysis from this study, the following conclusion can be made for the EPS-ferrocement geomat:

i. The density of EPB10 and EPB30 EPS-ferrocement geomat is respectively 2165 kg/m^3 and 1876 kg/m^3. The mass of both EPB10 and EPB30 geomat ranges from 4 kg to 4.2 kg which are considerably light.

ii. The EPB10 EPS-ferrocement geomat has compressive strength about 4.14 MPa to 4.23MPa which is about 16.7% to 17.1% of the compressive strength of 50mm × 50mm ×50mm of its mortar cube at 14th day strength. The EPB30 EPS-ferrocement geomat has compressive strength about 4.21 MPa to 5.5 MPa which is about 44.3% to 66.0% of the compressive strength of 50mm × 50mm ×50mm of its mortar cube at 14th day strength.

iii. The first crack flexural force of the EPB10 EPS-ferrocement geomat is about 1.27 kN to 1.69 kN and ultimate flexural force of about 5.66 kN to 6.76 kN. The first crack flexural force of the EPB30 EPS-ferrocement geomat is about 3.09 kN to 3.76 kN and ultimate flexural force of about 6.17 kN to 8.21 kN. The failure mode is due to flexural moment in the tension zone of 8-shaped geomat.

iv. It is believed that the EPS-ferrocement geomat has the potential to have higher compressive strength and flexural force value if they were casted in mold that can give them smooth finish and uniform dimension.

v. The pull out resistance force value, R of the single arrangement of EPB10 and EPB30 EPS-ferrocement geomat embedded in sandy soil under overburden pressure, P_o can be represented by $R = 0.234P_o + 0.765$ and $R = 0.271P_o + 0.43$ respectively.

The EPS-ferrocement geomat has similar compressive strength, lower value of tension force and pull out resistance in sandy soil under similar overburden load as compared to ferrocement geomat, used tires geomat and fiberglass geomat

REFERENCES

ACI 1999. ACI manual of concrete practice, American Concrete Institute.

ACI COMMITTEE 2003. Guide for structural lightweight aggregate concrete. ACI 213R-03, Farmington Hills, Mich.

ALEX, A. A. R. 2011. Soil Improvement using Ferrocment Geomat. University Sains Malaysia

BS 1983. Testing Concrete, Part 108, Method for Making Test Cubes from Fresh Concrete. British Standards Institution, London.

EN, B. 1999. 1015-3: 1999. Methods of test for mortar for masonry part 3: Determination of consistence of fresh mortar (by flow table).

GRAY, D. H. & SOTIR, R. B. 1996. Chapter 1 Introduction to Biotechnical Stabilization. Biotechnical and soil bioengineering slope stabilization: a practical guide for erosion control. Wiley-Interscience.

KAN, A. & DEMIRBOĞA, R. 2007. Effect of cement and EPS beads ratios on compressive strength and density of lightweight concrete. Indian journal of engineering & materials sciences, 14, 158-162.

LEKHA, K. R. 2004. Field instrumentation and monitoring of soil erosion in coir geotextile stabilised slopes—A case study. Geotextiles and Geomembranes, 22, 399-413.

MATTHEW STOVALL, P. & KING, B. 2011. Geosynthetics in Articulating Concrete Block Section Design.

NATIONAL ACADEMY OF SCIENCES, A. H. P. O. T. U. O. F. I. D. C. & ASSISTANCE, U. S. A. F. I. D. B. F. T. 1976. Chapter 2 Background Information. Ferrocement: applications in developing countries. National Academies.

PARK, S. G. & CHISHOLM, D. 1999. Polystyrene aggregate concrete. BRANZ.

SARADHI BABU, D., GANESH BABU, K. & WEE, T. H. 2005. Properties of lightweight expanded polystyrene aggregate concretes containing fly ash. Cement and Concrete Research, 35, 1218-1223.

XU, Y., JIANG, L., XU, J. & LI, Y. 2012. Mechanical properties of expanded polystyrene lightweight aggregate concrete and brick. Construction and Building Materials, 27, 32-38.

YOHANES, B. S. 2010. Rubberise Geo-Mat for Soil Improvement. University Sains Malaysia.